Article

Cell Reports

Non-canonical Binding Site for Bacterial Initiation Factor 3 on the Large Ribosomal Subunit

Graphical Abstract

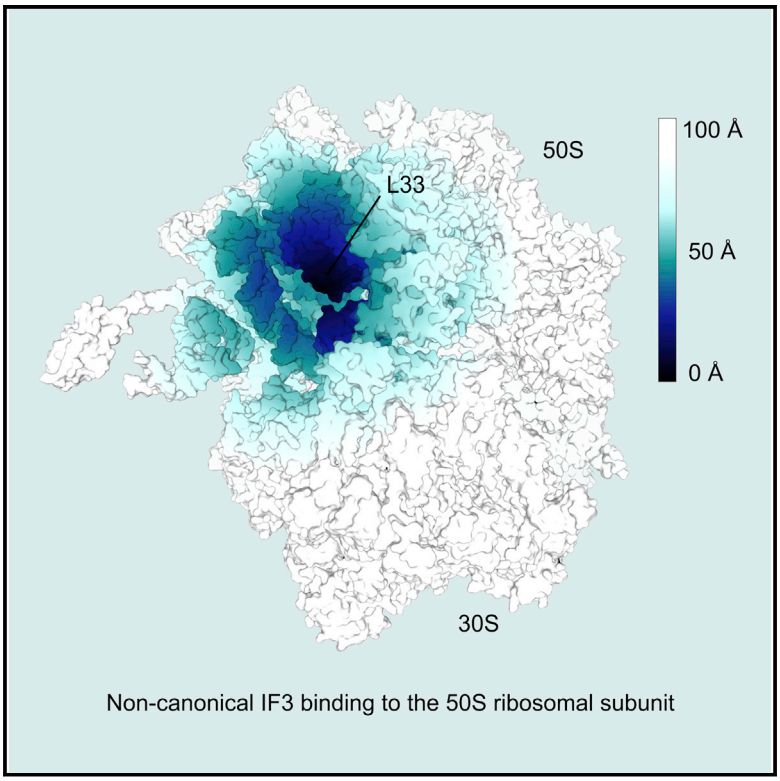

Non-canonical IF3 binding to the 50S ribosomal subunit

Authors

Akanksha Goyal, Riccardo Belardinelli, Marina V. Rodnina

Correspondence

rodnina@mpibpc.mpg.de

In Brief

Goyal et al. show that translation initiation factor 3 (IF3) has a binding site on the 50S ribosomal subunit. The interaction is predominantly electrostatic with very high rates of IF3 binding and dissociation. The binding may be implicated in alternative initiation modes performed directly by the 70S ribosomes.

Highlights

- Initiation factor 3 (IF3) can remain bound to the 70S IC after subunit joining
- IF3 binds to the 50S subunit near the ribosomal protein L33
- The interaction is largely electrostatic with high association and dissociation rates
- The interaction may be physiologically relevant for non-canonical initiation pathways

Goyal et al., 2017, Cell Reports *20*, 3113–3122
September 26, 2017
http://dx.doi.org/10.1016/j.celrep.2017.09.012

CellPress

Cell Reports
Article

Non-canonical Binding Site for Bacterial Initiation Factor 3 on the Large Ribosomal Subunit

Akanksha Goyal,[1] Riccardo Belardinelli,[1] and Marina V. Rodnina[1,2,*]
[1]Department of Physical Biochemistry, Max Planck Institute for Biophysical Chemistry, Am Fassberg 11, Goettingen 37077, Germany
[2]Lead Contact
*Correspondence: rodnina@mpibpc.mpg.de
http://dx.doi.org/10.1016/j.celrep.2017.09.012

SUMMARY

Canonical translation initiation in bacteria entails the assembly of the 30S initiation complex (IC), which binds the 50S subunit to form a 70S IC. IF3, a key initiation factor, is recruited to the 30S subunit at an early stage and is displaced from its primary binding site upon subunit joining. We employed four different FRET pairs to monitor IF3 relocation after 50S joining. IF3 moves away from the 30S subunit, IF1 and IF2, but can remain bound to the mature 70S IC. The secondary binding site is located on the 50S subunit in the vicinity of ribosomal protein L33. The interaction between IF3 and the 50S subunit is largely electrostatic with very high rates of IF3 binding and dissociation. The existence of the non-canonical binding site may help explain how IF3 participates in alternative initiation modes performed directly by the 70S ribosomes, such as initiation on leaderless mRNAs or re-initiation.

INTRODUCTION

Initiation is the most regulated step of protein synthesis during which the "translation potential" of an mRNA is assessed. The ribosome assembles on the mRNA start codon contained in a given sequence context, thus selecting the open reading frame for translation. In the canonical initiation pathway, the initiation factors (IF1, IF2, and IF3), mRNA and fMet-tRNA^{fMet} bind the small ribosomal subunit (30S) to form a 30S pre-initiation complex (30S PIC), which subsequently matures into a 30S IC upon start codon-anticodon recognition between the mRNA and fMet-tRNA^{fMet}. Thereafter, the docking of the large subunit (50S) activates GTP hydrolysis by IF2, the three IFs dissociate and fMet-tRNA^{fMet} accommodates into the P site of the ribosome, resulting in a 70S initiation complex (70S IC), which can take part in the next stage of elongation (reviewed in Gualerzi and Pon, 2015; Laursen et al., 2005; Milón and Rodnina, 2012).

Each phase of initiation is dynamic with respect to the composition of the complex as well as conformational and spatial rearrangements of the IFs, fMet-tRNA^{fMet}, and the ribosome. The IFs and fMet-tRNA^{fMet} influence the binding of one another to the 30S subunit by direct interactions or by indirectly modulating the structure of the complex (Goyal et al., 2015; Hussain et al., 2016; Milón et al., 2008, 2010, 2012). IF1 is a compact protein that binds to the A site on the 30S subunit (Carter et al., 2001; Sette et al., 1997) where it interacts with both IF2 and IF3, stabilizing them on the ribosome as well as enhancing their functions (Antoun et al., 2006a, 2006b; Hussain et al., 2016; Milón et al., 2012). IF2, a multi-domain translational GTPase, binds the formyl moiety of fMet-tRNA^{fMet} through its C-terminal C2 domain, thereby recruiting it to the ribosome (Guenneugues et al., 2000; Milón et al., 2010; Simonetti et al., 2008; Spurio et al., 2000). IF3 is comprised of two globular domains (N- and C-terminal [NTD and CTD, respectively]) separated by a flexible, positively charged linker region (Hussain et al., 2016; Kycia et al., 1995; Moreau et al., 1997). The factor extensively changes its position on the 30S subunit during initiation (Hussain et al., 2016). Before fMet-tRNA^{fMet} binding, IF3-NTD binds near the 30S platform while the CTD is positioned at the P site of the 30S subunit, whereas after fMet-tRNA^{fMet} binding and start codon recognition, the NTD moves to interact with the tRNA elbow and the CTD is displaced from the P site (Hussain et al., 2016). IF3 prevents premature subunit association by sterically blocking the binding site for Helix 69 (H69) in the 23S rRNA of the 50S subunit (Dallas and Noller, 2001; Julián et al., 2011). Whereas the simultaneous binding of GTP and fMet-tRNA^{fMet} confers an "active" conformation of IF2 which promotes rapid subunit joining (Antoun et al., 2003; Grunberg-Manago et al., 1975; Pavlov et al., 2011; Wang et al., 2015; Zorzet et al., 2010), IF3 induces an anti-association conformation of the 30S subunit, which is enhanced or alleviated depending on the mRNA sequence and correct start codon-anticodon interaction (Antoun et al., 2006b; Grigoriadou et al., 2007b; Milón et al., 2008). The antagonistic interplay between IF2 and IF3 fine-tunes the initiator tRNA selection and subunit joining, maintaining the balance between the speed and accuracy of initiation (Antoun et al., 2006b; MacDougall and Gonzalez, 2015).

The maturation of the 30S IC to an elongation-ready 70S IC involves a 50S subunit binding step, a chemical GTP hydrolysis step and several factor dissociation events that occur on the millisecond to second timescale. After subunit joining, GTP hydrolysis by IF2 is triggered leading to the release of fMet-tRNA^{fMet} from the C2 domain of the factor and into the P-site of the 70S IC, followed by the dissociation of IF1 and IF2 (Goyal et al., 2015; Grigoriadou et al., 2007a; Milón et al., 2008; Tomsic et al., 2000). Because IF3 binds to the principal inter-subunit bridges B2a and B2b, which are essential for stable subunit association (Dallas and Noller, 2001; Julián et al., 2011; Liu and Fredrick, 2015), stepwise docking of

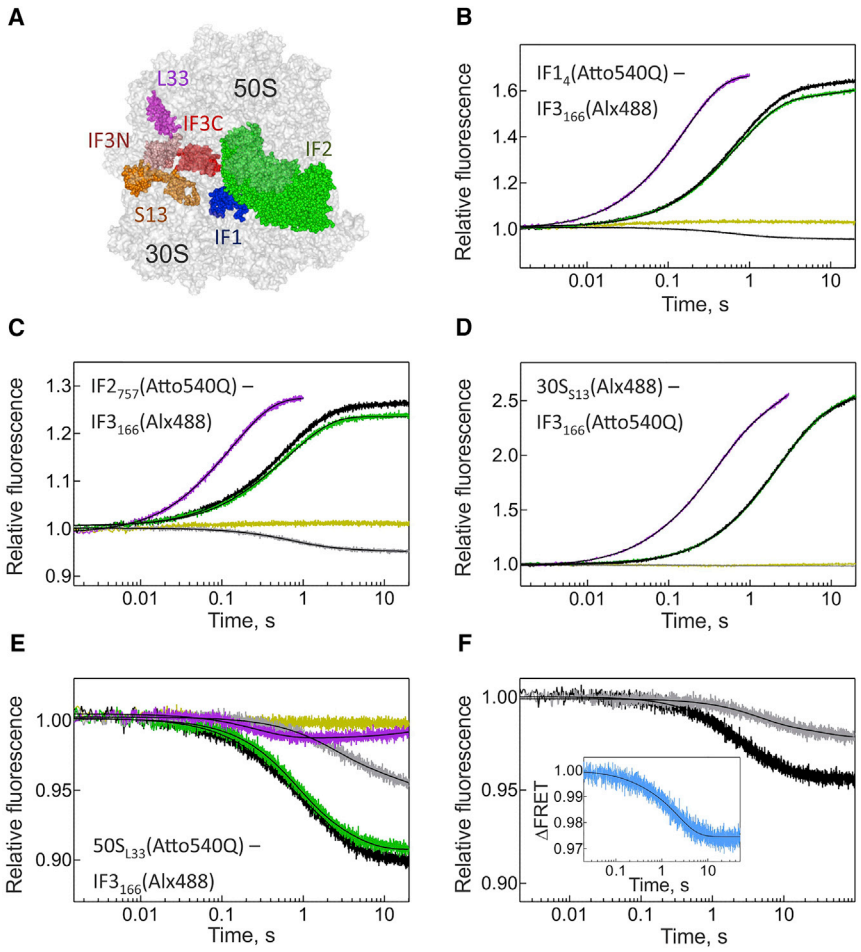

Figure 1. IF3 Dynamics during 70S IC Formation

(A) Location of the labeled proteins on the ribosome.

(B–E) Time courses with the indicated labeled components upon subunit joining. 30S IC (0.05 μM) was rapidly mixed with 50S subunits (0.15 μM) or unlabeled IF3 (1.5 μM, purple) in a stopped-flow apparatus and the FRET change between indicated components was monitored with time. The reactions were carried out at 20°C in buffer TAKM$_7$ in the presence of GTP (black), GTPγS (green), as well as in the absence of the 50S subunit (gold) or acceptor dye (gray). Time courses were fit using an exponential function (see Table S1 for rates). Fits are shown as black smooth lines.

(F) Lack of IF3 dissociation from the 70S IC. 30S IC containing IF3$_{166}$(Alx488) (0.075 μM) was rapidly mixed with unlabeled 50S (gray) or 50S$_{L33}$(Atto540Q) subunits (black) (0.075 μM). Fit of the time course obtained in the absence of the acceptor dye was subtracted from the trace obtained in its presence (inset).

See also Figures S1–S3 and Table S1.

RESULTS

IF3 Movements during Late Stages of Initiation

To monitor IF3 movements on the ribosome from different perspectives, we labeled initiation factors (IF1 at position 4, IF2 at position 757 and IF3 at position 166) as well as ribosomal proteins (S13 and L33) with fluorescent dyes Alexa(Alx) 488 or Atto540Q. We probed the neighborhood of IF3 using four FRET pairs (Figure 1A): IF1$_4$(Atto540Q)-IF3$_{166}$(Alx488), IF2$_{757}$ (Atto540Q)-IF3$_{166}$(Alx488), 30S$_{S13}$(Alx488)-IF3$_{166}$(Atto540Q), and 50S$_{L33}$(Atto540Q)-IF3$_{166}$(Alx488); subscripts denote labeling positions. Close proximity between two ligands labeled with the donor dye (Alx488) and the non-emitting acceptor dye (Atto540Q), respectively, should result in fluorescence quenching. When we rapidly mixed labeled 30S PIC (lacking IF3) with labeled IF3 in a stopped-flow machine, a large decrease in fluorescence (30%–60%) was observed upon binding (Figure S1). Control reactions performed in the absence of the acceptor dye resulted in a negligible fluorescence change of the donor alone. Because fluorescence labeling can adversely affect the function of a protein, we checked the activity of each reporter in promoting subunit joining by light scattering and found it to be comparable with that of its unlabeled counterpart (Figure S2).

We next prepared dual-fluorescence labeled 30S ICs containing labels on IF3 on one hand, and on IF1, IF2, or the ribosomal protein S13 on the other hand, in the presence of GTP, and rapidly mixed each type of complex with a 3-fold excess of unlabeled 50S subunits (Figures 1B–1D). Alternatively, we rapidly mixed single-labeled 30S IC containing IF3$_{166}$(Alx488) with a 3-fold excess of 50S$_{L33}$(Atto540Q) (Figure 1E). Subunit joining the 50S subunit concomitantly displaces IF3 from its binding site on the 30S subunit (Elvekrog and Gonzalez, 2013; Fabbretti et al., 2007; Milón et al., 2008). However, structural studies of the 70S IC prepared in the presence of all IFs and a non-hydrolysable analog of GTP revealed a density in the 70S complex, which was attributed to IF3 (Allen et al., 2005). In addition, recent studies implicated the 70S-bound IF3 in mediating initiation of leaderless mRNAs as well as inducing a post-termination 70S-scanning mode for re-initiation (Yamamoto et al., 2016). These observations suggest the presence of an IF3 binding site on the 70S ribosome, which does not sterically hinder subunit association.

In this work, we follow IF3 dynamics after subunit joining using fluorescence-based rapid ensemble kinetics. We have utilized a highly purified in vitro reconstituted system of translation initiation from *Escherichia coli*, which contains fluorescence-labeled initiation factors and ribosomal subunits. IF3 movement with respect to other components of the initiation machinery was monitored in real-time by recording fluorescence resonance energy transfer (FRET) efficiency changes. Using this approach, we have identified a transient attachment of IF3 to the 50S subunit, which is largely mediated by electrostatic interactions.

was monitored via changes in light scattering (Figure S3), while the dynamics of IF3 with respect to other initiation components was followed by recording the signal changes of the fluorescence donor (Figure 1, black traces). Additionally, we performed control reactions in the absence of the acceptor dye (gray traces) or the 50S subunit (gold traces).

For all FRET pairs involving IF3 and the components of the 30S IC, we observed a fluorescence increase upon 50S subunit joining indicating that IF3 moves apart from its FRET partner on the 30S subunit (Figures 1B–1D). The amplitude of the fluorescence change was similar to that recorded upon chase of the labeled IF3 from the 30S complex (purple traces), suggesting that the factor either dissociates from the 70S IC or moves away from its original location on the 30S IC. 50S joining results in major rearrangements of the initiation complex and, in principle, a change in FRET efficiency can be caused not only by the movement of IF3, but also by rearrangements of IF2, IF1, or conformational changes of the 30S subunit. Notably, the conformational dynamics of IF2, as well as the coupled movements of IF1 and of the 30S subunit, are dependent on GTP hydrolysis, whereas the IF3 dynamics are not (Goyal et al., 2015). Hence, we also conducted experiments using a non-hydrolysable GTP analog, GTPγS (green traces), in place of GTP to suppress the IF2-IF1-related rearrangements, thereby ensuring that we monitored only IF3-related events. The reactions displayed negligible dependence on IF2-dependent GTP hydrolysis, and, in all cases, the apparent rates of fluorescence change were either similar to or slightly slower than the rate of subunit joining (see Table S1 for rates). We did not observe any FRET change upon dilution of the complexes with buffer indicating that the dual-labeled 30S ICs were stable. In the absence of the acceptor dye, fluorescence change of the donor amounted to less than 20% of the signal change observed in its presence, demonstrating a high FRET efficiency.

Surprisingly, when we mixed 30S IC formed with $IF3_{166}$(Alx488) with a 3-fold excess of $50S_{L33}$(Atto540Q), a decrease in fluorescence amplitude was observed (Figure 1E, black trace). The intrinsic donor fluorescence change of $IF3_{166}$(Alx488) accounted for 40% of the amplitude change (gray trace), whereas the rest could only be explained by fluorescence quenching due to the migration of IF3 in the vicinity of L33 on the 50S subunit. To discriminate whether the FRET is due to the movement of IF3 within the 70S IC or/and dissociation and subsequent re-binding of IF3 to the free 50S in solution, we minimized the amount of free 50S subunits by mixing the 30S IC with an equimolar concentration of unlabeled 50S or $50S_{L33}$(Atto540Q). The difference in the amplitude change between FRET and the donor fluorescence persisted (Figure 1F (inset)), indicating that a population of IF3 remains bound to the 70S IC. Thus, despite moving away from its canonical binding site on the 30S subunit, IF3 can remain bound to the 70S complex by interactions with a second, non-canonical site.

IF3 Specifically Binds to a Single Site on the 50S Subunit

We next investigated whether the second binding site for IF3 lies on the 50S subunit. For this purpose, we checked the binding of fluorescence-labeled IF3 directly to the labeled 50S subunit; labeling positions are depicted in Figure 2A. When we rapidly mixed $IF3_{166}$(Alx488) with $50S_{L33}$(Atto540Q), the interaction between the two ligands resulted in a significant quenching of the donor fluorescence (Figure 2B, black trace). In the absence of the acceptor dye, only a small change in donor fluorescence was recorded (gray trace). To the best of our knowledge, the observed interaction between IF3 and the 50S subunit has not been directly monitored before. Therefore, we carried out a series of control experiments to validate our finding. First, we performed similar experiments with IF2, which contacts the 50S subunit upon docking and thus might form a complex with the isolated 50S subunit. Upon mixing $IF2_{757}$(Alx488) with $50S_{L33}$(Atto540Q) (Figure 2B, dark blue trace), we observed no fluorescence change, which indicated that the interaction was specific to IF3. Second, there was no fluorescence change upon mixing $IF3_{166}$(Alx488) with the isolated ribosomal protein L33(Atto540Q) (light blue trace), suggesting that the binding of IF3 was specific to the 50S subunit. Third, to ensure that the interaction can also be detected using a conventional FRET pair containing an emitting acceptor dye, we mixed $IF3_{166}$(Alx488) with $50S_{L33}$(Atto565) (Figure 2C) and observed an increase in the acceptor fluorescence signal, whereas $50S_{L33}$(Atto565) did not change fluorescence when mixed with unlabeled IF3. Fourth, we confirmed that the interaction was not limited to IF3 coupled with Alx488 by swapping the fluorescent labels on IF3 and the 50S subunit (Figure 2D). Finally, we made sure that the interaction could be observed from a different position on IF3 by performing similar experiments with IF3 labeled at residue 65 on the NTD ($IF3_{65}$(Alx488)) and $50S_{L33}$(Atto540Q) (Figure 2E).

We also checked the specificity of the interaction using the fluorescence quenching signal generated upon binding of $IF3_{166}$(Alx488) to $50S_{L33}$(Atto540Q). Because the reaction was extremely fast (Figure 2F, black trace), such that a significant portion of the amplitude was lost during the dead time of the stopped-flow machine (1.5 ms), we compared the fluorescence signal of each trace with the fluorescence of $IF3_{166}$(Alx488) alone (Figure 2F, gold trace), which corresponds to the true fluorescence of the sample at time 0. When $50S_{L33}$(Atto540Q) was pre-incubated with excess amounts of IF1, a positively charged protein with an isoelectric point similar to that of IF3 (pI_{calc} = 9.2 and 9.5, respectively), $IF3_{166}$(Alx488) binding was not affected, reaffirming the existence of a distinct IF3 binding site (Figure 2F, pink trace). Also addition of excess mRNA had hardly any effect on IF3 recruitment (orange trace), suggesting that the binding was not principally mediated by non-specific interactions of IF3 with rRNA. Thus, we concluded that IF3 binds to the 50S subunit in a specific manner.

To calculate the number of IF3 molecules that bind to the 50S subunit, we utilized the finding that the fluorescence anisotropy of $IF3_{166}$(Alx488) increases upon binding to unlabeled ribosomal subunits (Figure 3A). We titrated a fixed concentration of $IF3_{166}$(Alx488) with sub- and over-stoichiometric amounts of 50S subunits (Figure 3B) and obtained a value of $\sim$1.2 IF3 molecules per 50S subunit. This value is indicative of one specific binding site for IF3 on the 50S subunit; the slight deviation of 1:1 binding stoichiometry may be attributed to difficulties in estimating the active concentrations precisely.

Furthermore, we determined the affinity of IF3 binding to the 50S subunit by rapidly mixing $IF3_{166}$(Alx488) with increasing amounts of $50S_{L33}$(Atto540Q). To measure the temperature

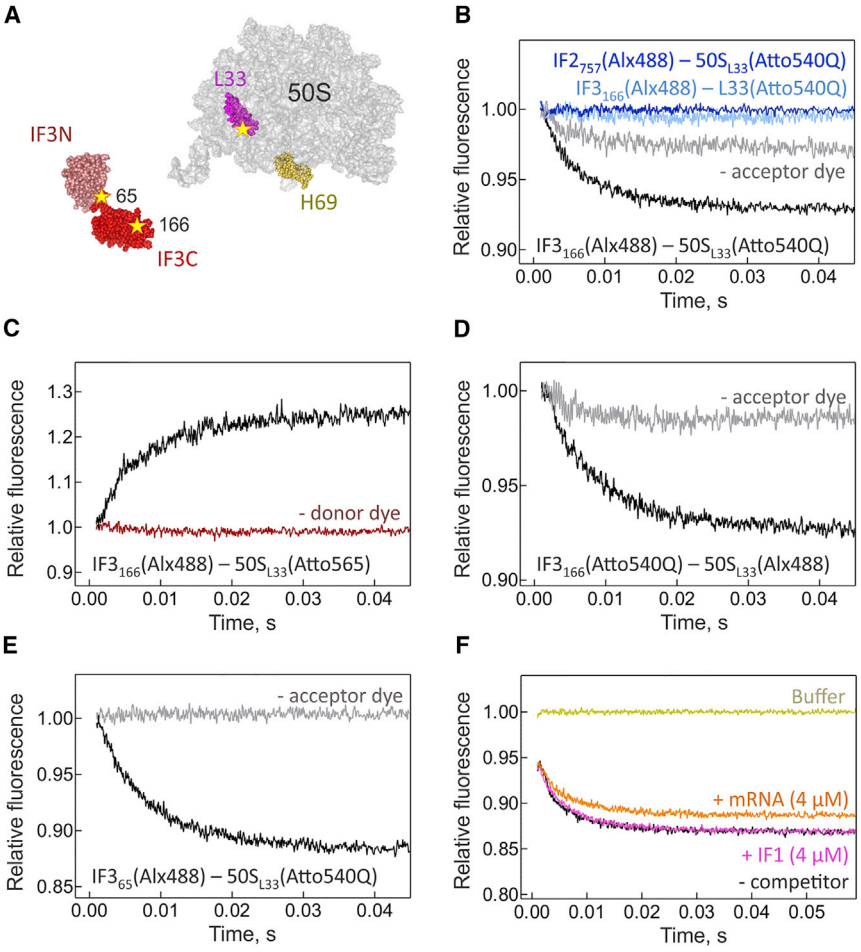

Figure 2. IF3 Interaction with the 50S Subunit Monitored Using Different Fluorescent Reporters

All reactions were carried out in buffer $TAKM_7$ at 4°C.

(A) Fluorescence-labeled positions on IF3 and the 50S subunit.

(B–E) Time courses with the indicated labeled components. Labeled IF3 (0.05 μM) was rapidly mixed with labeled 50S subunits (0.075 μM), and FRET changes were followed with time. Control measurements were performed in the absence of the donor (brown) or acceptor dye (gray).

(F) The specificity of the IF3–50S subunit interaction. $IF3_{166}$(Alx488) (0.05 μM) and $50S_{L33}$(Atto540Q) (0.075 μM) were rapidly mixed in the presence of excess IF1 or mRNA. Control measurements were performed without any 50S subunits (gold) or in the absence of any competitor (black).

dependence of the reaction kinetics, we performed experiments at 4°C (Figure 4A) and 20°C (Figure 4B). To calculate the dissociation rate of IF3 from the 50S subunit, we formed a complex of $IF3_{166}$(Alx488) with $50S_{L33}$(Atto540Q) and then rapidly mixed it with a 5- or 10-fold excess of unlabeled 50S subunits or wild-type (WT) IF3, respectively (Figures 4C and 4D). A rapid increase in fluorescence was observed upon chase indicative of dissociation of the complex. Global fitting of binding and dissociation time courses, obtained at 4°C or 20°C, to a one-step association-dissociation model yielded an association rate constant (k_{on}) of 1,300 ± 100 μM^{-1} s^{-1} or 1,900 ± 100 μM^{-1} s^{-1}, respectively, and a dissociation rate constant (k_{off}) of 80 ± 10 s^{-1} or 160 ± 10 s^{-1}, respectively, demonstrating that the interaction is highly labile. The K_D values estimated from k_{on} and k_{off} are 60 ± 10 nM and 90 ± 10 nM at 4°C and 20°C, respectively, indicating that the binding affinity displays a slight dependence on the temperature.

Because site-directed mutagenesis and subsequent fluorescence labeling can alter binding affinities of biomolecules, we determined the affinity of the unlabeled native IF3 (IF3 WT) to the 50S subunit at 4°C by rapidly mixing $IF3_{166}$(Alx488) with $50S_{L33}$(Atto540Q) that was pre-incubated with unlabeled IF3 WT (Figure 4E). The degree of binding inhibition calculated from the decrease in fluorescence change was plotted against increasing IF3 WT concentrations (Figure 4F) and yielded an IC_{50} of 0.6 ± 0.2 μM and a corresponding K_i of 0.3 ± 0.1 μM. The K_i value is higher than the K_D of the $IF3_{166}$(Alx488)-50S subunit complex estimated from the k_{on} and k_{off} values, but within a reasonable concentration range, given the experimental uncertainties in estimating active concentrations of IF3. We also tested competition by a mixture of individual domains of IF3 and observed a 27% inhibition (Figure 4E), as compared to 77% inhibition at equivalent concentrations of full-length IF3 WT (interpolated from Figure 4F). This suggests that (1) the individual domains have a lower affinity to the 50S subunit as compared to the full-length protein (as was shown for the 30S subunit [Petrelli et al., 2001]) or/and (2) the binding may be mediated partially by the positively charged lysine-rich linker region, which connects the two domains.

IF3 Binding to the 50S Subunit Is Mediated by Electrostatic Interactions

Next, we proceeded to investigate the nature of the interaction between IF3 and the 50S subunit. All experiments presented thus far were performed in the standard buffer $TAKM_7$ (20 mM Tris-HCl [pH 7.5], 30 mM KCl, 70 mM NH_4Cl, and 7 mM $MgCl_2$). The fluorescence change depicting the binding was abolished when the $MgCl_2$ concentration was increased to 20 mM ($TAKM_{20}$, Figure 5A). Replacing NH_4Cl with KCl ($TK_{100}M_7$) did not affect the interaction. However, the extent of binding was highly sensitive to the KCl concentration: a much greater amplitude change was observed at 50 mM ($TK_{50}M_7$) than at 100 mM KCl, whereas at 200 mM KCl ($TK_{200}M_7$) the interaction was completely inhibited. Such a salt dependence is strongly indicative of electrostatic interactions. We also tested

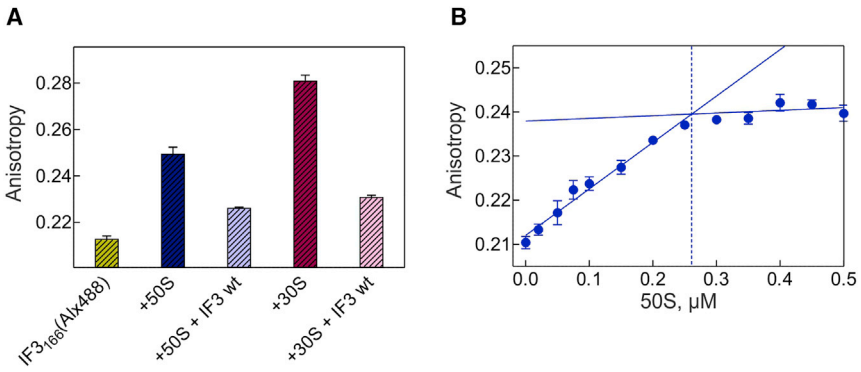

Figure 3. Stoichiometry of IF3 Binding to the 50S Subunit

(A) Changes in fluorescence anisotropy of $IF3_{166}$(Alx488) upon binding to ribosomal subunits. The fluorescence anisotropy of $IF3_{166}$(Alx488) (0.015 μM) alone, in the presence of 50S or 30S (0.3 μM), and upon chase with unlabeled IF3 wild-type (WT) was measured at equilibrium conditions using a spectrofluorometer.

(B) The stoichiometry of IF3 binding to the 50S subunit. The fluorescence anisotropy of $IF3_{166}$(Alx488) (0.3 μM) was measured upon incubation with different amounts of 50S subunits (see Experimental Procedures for details of fitting). All reactions were carried out in buffer $TAKM_7$ at 20°C. Error bars depict the SD of the mean of three technical replicates.

the reaction in buffer containing 100 mM potassium glutamate (KGlu) ($T[KGlu]_{100}M_7$), the major intracellular ionic osmolyte in *E. coli*, and observed a larger fluorescence change than with KCl (Figure 5B). This is in accordance with reports that have shown that replacing KCl with KGlu enhances protein-nucleic acid interactions (Deredge et al., 2010; Leirmo et al., 1987; Menetski et al., 1992).

We further characterized the dependence of the interaction on different salt concentrations by pre-incubating $IF3_{166}$(Alx488) with saturating amounts of 50S subunits in a low salt buffer ($TK_{20}M_7$) to form a complex and then measuring changes in fluorescence anisotropy at increasing concentrations of NaCl, KCl, KGlu, or $MgCl_2$ (Figure 5C). We observed that, although the dependence of the IF3-50S subunit interaction on sodium and potassium chloride concentrations was similar (IC_{50} ~80–85 mM added salt), the binding persisted at much higher amounts of potassium glutamate (IC_{50} ~215 mM). We also observed that Mg^{2+} was significantly more potent in disrupting the interaction than the monovalent salts (IC_{50} ~20 mM). Hence, taking into consideration the concentration of IF3 in vivo, 1–4 μM (Gualerzi and Pon, 1990; Howe and Hershey, 1983), as well as the cellular osmotic environment with its high levels of potassium glutamate and low levels of free magnesium and chloride, the interaction between IF3 and the 50S subunit is expected to be rather strong inside the cell.

DISCUSSION

The timing and extent of IF3 dissociation upon transition from the 30S IC to 70S IC has been a source of considerable discussion. Because the location of IF3 at the subunit interface occludes 50S subunit joining by hindering the establishment of inter-subunit bridge B2a-b, it is generally accepted that IF3 must eventually dissociate from its binding site on the 30S subunit to allow stable subunit association. The initial suggestion that IF3 dissociates from the 30S subunit after start codon recognition, but before subunit joining, owing to a decrease in affinity toward the correctly formed 30S IC (Antoun et al., 2006b), has been refuted by several reports, which showed that IF3 remains tightly bound to the 30S IC until after 50S subunit docking. These studies followed IF3 dynamics with respect to other components of the 30S IC, i.e., (1) monitored the loss of FRET between IF3 and fMet-$tRNA^{fMet}$ upon subunit association (Goyal et al., 2015; Milón et al., 2008); (2) compared the initiation kinetics with mRNAs varying in the identity of the start codon (Grigoriadou et al., 2007b); (3) followed IF3 dynamics using time-resolved chemical probing (Fabbretti et al., 2007); and (4) studied the effects of deleting H69 on IF3 dissociation via FRET between IF3 and the 30S subunit or fMet-$tRNA^{fMet}$ (Liu and Fredrick, 2015). A recent report on non-canonical initiation pathways such as leaderless initiation and re-initiation (Yamamoto et al., 2016) also showed that IF3 can bind to different 70S complexes. However, direct evidence demonstrating and characterizing the binding site on the 70S ribosome has remained scarce.

Consistent with previous reports (Goyal et al., 2015; Liu and Fredrick, 2015; Milón et al., 2008), we observe that IF3 does indeed move away from its binding site on the 30S subunit as well as 30S-bound factors IF1 and IF2 upon subunit association. The timing of IF3 displacement in each case is slightly slower than that of 50S joining (Table S1) but must precede the subsequent IF1 and IF2 release because the dissociation of the latter factors depends on GTP hydrolysis (Goyal et al., 2015), whereas IF3 dynamics are not affected when GTP is replaced with a non-hydrolysable analog. Remarkably, we find that IF3 moves toward the 50S subunit, into the proximity of the fluorescence-labeled L33 located near the E site of the ribosome. We note, however, that there were no free 30S subunits present in these experiments. Inside the cell, where a fraction of the ribosomes is split into subunits, the proportion of IF3 that remains bound to the 70S IC may be reduced due to its sequestration by free 30S subunits, which have a very high affinity for IF3 (Milón et al., 2012; Weiel and Hershey, 1981).

We show that IF3 can bind to free 50S subunits in solution. At 20°C, the association is very fast (1,900 μM^{-1} s^{-1}), similar to IF3 binding to the 30S subunit (1,160 μM^{-1} s^{-1} [Milón et al., 2012]). However, in contrast to the 30S subunit, which binds IF3 in a stable manner (k_{off} = ~1 s^{-1} [Milón et al., 2012]), IF3 association with the 50S is highly labile, with a rapid dissociation rate constant of 160 s^{-1}. The high dissociation rate explains why the IF3-50S complex is difficult to characterize using traditional assays such as pull-down and gel filtration. While some studies showed that IF3 and 50S subunit interact with one another using sucrose density-gradient centrifugation, the authors did not discuss the phenomenon (Ayyub et al., 2017; Hirokawa et al., 2007). Early

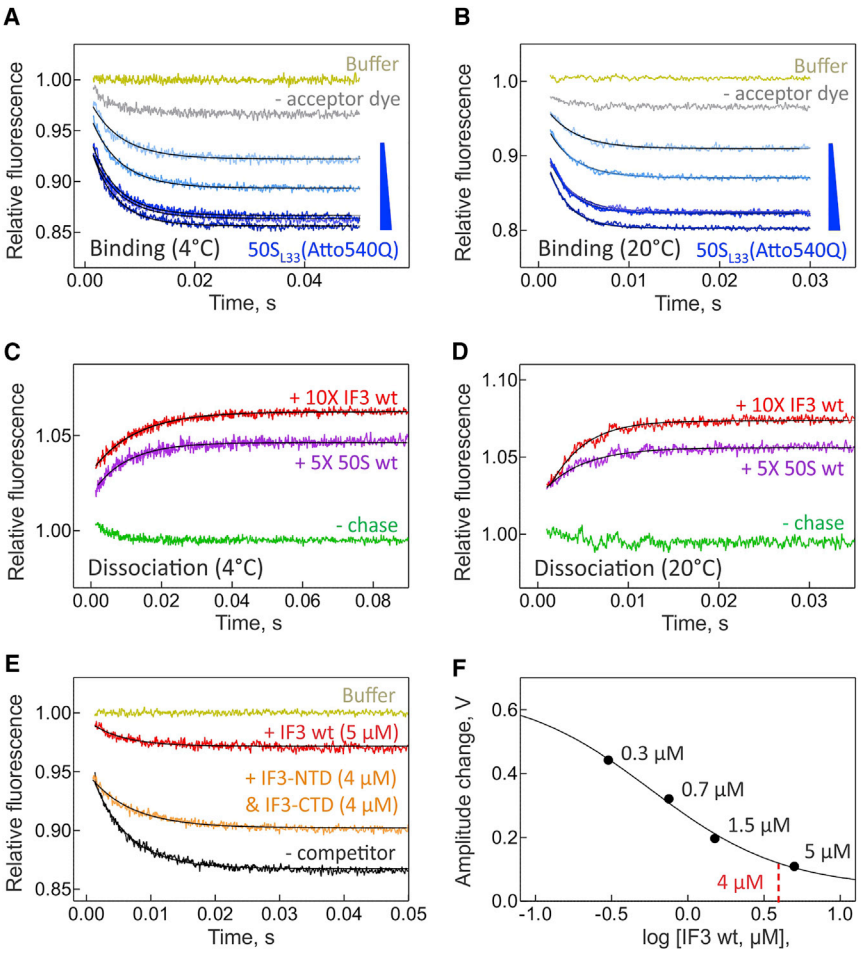

Figure 4. IF3 Binding and Dissociation Kinetics with the 50S Subunit

(A and B) Binding of IF3$_{166}$(Alx488) (0.05 μM) to increasing concentrations of 50S$_{L33}$(Atto540Q) subunits (0.05 – 0.15 μM) at 4°C (A) and 20°C (B). Control measurements were performed in the absence of 50S subunits (gold) or acceptor dye (gray).

(C and D) Dissociation of IF3$_{166}$(Alx488) (0.15 μM) from 50S$_{L33}$(Atto540Q) (0.05 μM) at 4°C (C) and 20°C (D), upon chase with 5- or 10-fold excess of unlabeled 50S or IF3 WT, respectively. Control measurements were performed in the absence of unlabeled competitor (green). Time courses were fit using numerical integration. All fits are shown as smooth black lines.

(E) Binding of IF3$_{166}$(Alx488) (0.05 μM) to 50S$_{L33}$(Atto540Q) (0.075 μM) in the presence of excess unlabeled IF3 WT or a mixture of individual IF3 domains at 4°C. Control measurements were performed without any 50S subunits (gold) or in the absence of any competitor (black). Time courses were evaluated by a single-exponential function. All fits are shown as smooth black lines.

(F) The dependence of the total fluorescence amplitude change of the raw stopped-flow traces upon IF3$_{166}$(Alx488) (0.05 μM) binding to 50S$_{L33}$(Atto540Q) (0.075 μM) on increasing concentrations of unlabeled IF3 WT (see Experimental Procedures for details of fitting). All reactions were performed in buffer TAKM$_7$. Error bars represent the standard error of the fit and are not visible due to a smaller size than of the symbol.

studies detected crosslinks between IF3 and the ribosomal proteins L2, L5, and L17 (Chaires et al., 1982) or L2, L7/L12, L11, and L27 (Schwartz et al., 1983), but the discrepancy between the ribosomal proteins implicated in binding IF3 in the two studies, as well as their scattered locations on the 50S surface, warrant some caution in interpreting these findings.

The binding of IF3 to the 50S subunit relies on electrostatic interactions and is inhibited at high salt concentrations, with the potency of different salts decreasing in the following order: $MgCl_2$ > KCl = NaCl > KGlu. The rapid association and dissociation constants, as well as the significant electrostatic component of binding, are characteristic of sequence- or conformation-unspecific interactions, which are facilitated largely by the oppositely charged potential of binding partners. Such interactions are omnipresent in nature; for instance, they exist between DNA-repair enzymes and undamaged DNA sequences (Cravens et al., 2014) as well as chaperones and correctly folded proteins (Koldewey et al., 2016). Facilitated by long-range electrostatic interactions, the enzyme rapidly binds different substrates, but the complex is stabilized only when the initial binding is followed by a second step where additional short-range interactions are formed (Meneses and Mittermaier, 2014). If such rearrangements do not take place, the complex rapidly dissociates and the enzyme resumes the sampling of other targets. In other cases, sequence-unspecific binding of genome regulatory proteins to DNA (Berg et al., 1981), as well as of ricin ribotoxin to the bacterial ribosome (Korennykh et al., 2006), accelerates the process of locating the sequence-specific binding site via one- or two-dimensional diffusion. These are examples of nucleic acid-binding proteins, which often have a pI >9 and bind to multiple sites on the large surface area of the negatively charged substrate. The binding of IF3 to the 50S subunit is unique in the sense that IF3 distinctly binds to a single site on the 50S subunit, somewhere in the vicinity of L33. Additionally, whereas the difference between affinities toward sequence-specific and sequence-unspecific binding sites typically ranges from 10^4- to 10^7-fold (Saecker, 2007), IF3 binding to the 50S subunit is only a 100-fold weaker than to its canonical site on the 30S subunit ($K_{D,\ IF3\text{-}50S}$ = 0.3 μM [this work]; $K_{D,\ IF3\text{-}30S}$ = 0.003 μM [Milón et al., 2012]).

Although IF3 has a distinct binding site on the 50S subunit, the transient nature of binding and the availability of free 30S subunits in vivo make it unlikely that the interaction with free 50S subunits is prevalent at normal growth conditions. One attractive possibility is that the non-canonical 50S binding site is implicated in 70S-mediated initiation (Yamamoto et al., 2016). This possibility is supported by the finding that, while IF3 binding to

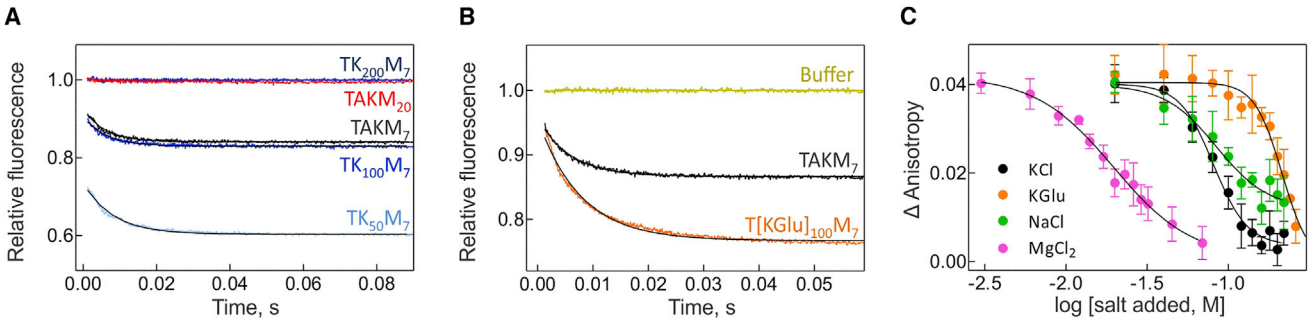

Figure 5. Electrostatic Interactions between IF3 and the 50S Subunit

(A and B) The effect of different $MgCl_2$ and KCl concentrations (A) or replacing potassium chloride with potassium glutamate (B) on IF3-50S subunit interaction. $IF3_{166}$(Alx488) (0.05 μM) and $50S_{L33}$(Atto540Q) (0.075 μM) were rapidly mixed under different buffer conditions at 4°C, and FRET changes were recorded with time. A control measurement performed in buffer $TAKM_7$ is depicted in both panels for comparison. Time courses were fit using a single-exponential function. Fits are shown as black smooth lines.

(C) Salt concentration dependence of IF3-50S subunit interaction. $IF3_{166}$(Alx488) (0.015 μM) was pre-incubated with 50S subunits (0.3 μM) in buffer $TK_{20}M_7$ and the decrease in anisotropy (depicting $IF3_{166}$(Alx488) dissociation from 50S subunits) upon increasing concentrations of the indicated salts was measured at 20°C. The data were corrected by subtracting the corresponding anisotropy measurements obtained with $IF3_{166}$(Alx488) alone (see Experimental Procedures for details about fitting). Error bars in (C) depict the SD of the mean of three technical replicates.

the 70S promotes initiation on leaderless mRNAs, binding of IF3 to the 30S subunit abolishes it (Yamamoto et al., 2016; unpublished data from our lab). Under cellular conditions where the concentrations of IF3 and of free ribosomal subunits are similar (Howe and Hershey, 1983; Mohapatra et al., 2017), IF3 preferentially binds to 30S subunits and participates in the canonical initiation process to form a high-fidelity 30S IC. However, under conditions where 70S monosomes accumulate (e.g., during cold-shock or deprivation of an energy source [Broeze et al., 1978; Moll et al., 2004; Ruscetti and Jacobson, 1972; Uchida et al., 1970]), IF3 concentration surpasses that of the 30S subunits (Giuliodori et al., 2007), or ribosomal recycling is mitigated (Hirokawa et al., 2004), IF3 binding to 70S monosomes may stimulate alternative modes of initiation involving leaderless mRNAs or allow existing 70S translation complexes to subsequently participate in re-initiation. Hence, the ratio between free subunits and IF3 is expected to be an important determinant for different initiation modes inside the cell.

EXPERIMENTAL PROCEDURES

Preparation of Components

Wild-type 30S and 50S subunits were prepared from *E. coli* MRE600 strain using zonal centrifugation (Rodnina et al., 1995). For re-activation, 30S subunits were incubated in buffer $TAKM_{20}$ (50 mM Tris-HCl [pH 7.5], 70 mM NH_4Cl, 30 mM KCl, 20 mM $MgCl_2$) for 30 min at 37°C. IF1, IF2, and IF3 were purified according to published protocols (Milón et al., 2007). f[^{3}H]Met-$tRNA^{fMet}$ was purified using HPLC (Milón et al., 2007), and the aminoacylation and formylation efficiency was >95%. 022 mRNA (Goyal et al., 2015; Milón et al., 2007) was prepared by T7 RNA-polymerase in vitro transcription and purified using Rneasy isolation kit (QIAGEN). GTP and GTPγS were purchased from Jena Biosciences.

Cysteine residues were introduced at position 4 in IF1, position 757 in IF2, and position 166 in IF3 and labeled with a thiol-reactive fluorescent donor (Alexa(Alx)488) or non-emitting acceptor (Atto540Q) dye using established protocols (Milón et al., 2007, 2012). 30S subunits that lacked the ribosomal protein S13 (30S ΔS13) and 50S subunits lacking L33 (50S ΔL33) were purified from *E. coli* K12 strain (Cukras and Green, 2005). 30S ΔS13 and 50S ΔL33 were reconstituted with fluorescence-labeled $S13_{112}$(Alx488) or fluorescence-labeled $L33_{31}$(Atto540Q or Alx488 or Atto565), respectively (Belardinelli et al., 2016; Caliskan et al., 2014). To prevent labeling at multiple positions, the native cysteine residues of each labeled protein were mutated to non-reactive serine residues. The efficiency of labeling and reconstitution was assessed as 90%–100% by absorbance measurements and SDS-PAGE analysis.

Stopped-Flow Kinetics

Stopped-flow measurements were performed with an SX-20MV stopped-flow machine (Applied Photophysics). All experiments were carried out in buffer $TAKM_7$ (50 mM Tris-HCl [pH 7.5], 70 mM NH_4Cl, 30 mM KCl, 7 mM $MgCl_2$), unless indicated otherwise. Because free IF3 has a propensity to stick to the walls of reaction tubes and optical cuvettes, all reactions were performed in the presence of 0.1 mg/mL BSA. To form 30S IC, 30S subunits (0.1 μM) were incubated with a 3-fold molar excess of unlabeled IF1, IF2, and equimolar amounts of $IF3_{166}$(Alx488), or a 2-fold excess of labeled $IF1_4$(Atto540Q) (Figure 1B), $IF2_{757}$(Atto540Q) (Figure 1C), or $IF3_{166}$(Atto540Q) (Figure 1D), as well as a 6-fold molar excess of mRNA and f[^{3}H]Met-$tRNA^{fMet}$ in buffer $TAKM_7$ containing GTP (0.25 mM) for 30 min at 37°C. To monitor IF3 dynamics during 70S IC formation, equal volumes (60 μL each) of fluorescence-labeled 30S IC (0.05 μM; all concentrations are final after mixing) and unlabeled 50S or $50S_{L33}$(Atto540Q) (0.15 μM) were rapidly mixed together at 20°C, and the fluorescence changes were recorded with time. To monitor IF3 binding to the 30S PIC (lacking IF3), fluorescent 30S PIC (0.05 μM) was rapidly mixed with an equimolar amount of fluorescence-labeled IF3. Release of labeled IF3 from the 30S IC was monitored by rapidly mixing fluorescent 30S IC (0.05 μM) with unlabeled IF3 (1.5 μM). Light scattering measurements were carried out without a filter by setting the excitation wavelength to 434 nm (Milón et al., 2008). Fluorescence change of Alx488 as well as FRET between Alx488 and Atto540Q were monitored upon excitation at 470 nm after passing through a KV500 cutoff filter (Schott). The averages of seven to ten time courses were evaluated by Prism (GraphPad Software) using exponential functions (Table S1).

The binding of IF3 to the 50S subunit was monitored by rapidly mixing the indicated combinations of fluorescence-labeled IF3 (0.05 μM) and fluorescent 50S subunits (0.075 μM) in a stopped-flow apparatus at 4°C in buffer $TAKM_7$, unless indicated otherwise. FRET between Alx488 and Atto565 was measured upon excitation at 470 nm, and the emission was monitored after passing through a KV590 cutoff filter (Schott). All data points in the time courses of the initial screening (Figures 2B–2E) were normalized with respect to the initial fluorescence of the time course observed after the dead time of the instrument (1.5 ms).

Inhibition of $IF3_{166}$(Alx488) binding to $50S_{L33}$(Atto540Q) was measured in the presence of increasing amounts of unlabeled IF3 WT (0.3–5 μM) or an 80-fold molar excess of unlabeled IF1, mRNA, or individual domains of IF3 over $IF3_{166}$(Alx488). The average of seven to ten time courses was evaluated using single-exponential function (GraphPad Prism software), and the total amplitude change from the raw stopped-flow data were plotted as a function of unlabeled IF3 WT concentration. The data were fit using the equation:

$$Y = y_0 + (y_1\text{-}y_0)/\left(1 + 10^{(\log(IC50 - x))}\right),$$

where, y_0 = minimum value; y_1 = maximum value; x = log of unlabeled IF3 WT concentration in μM; IC_{50} = inhibitory concentration corresponding to 50% of the amplitude change. The corresponding K_i value for IF3 WT was calculated using the equation:

$$K_i = IC_{50}/(1 + ([L]/K_D)),$$

where, K_i = inhibitory constant; [L] = $50S_{L33}$(Atto540Q) concentration; K_D = equilibrium dissociation constant of the $IF3_{166}$(Alx488)-$50S_{L33}$(Atto540Q) complex.

$IF3_{166}$(Alx488) binding to $50S_{L33}$(Atto540Q) was measured under five different buffer conditions besides $TAKM_7$ ($TAKM_{20}$; $TK_{100}M_7$ (50 mM Tris-HCl [pH 7.5], 100 mM KCl, 7 mM $MgCl_2$); $TK_{50}M_7$ (50 mM Tris-HCl [pH 7.5], 50 mM KCl, 7 mM $MgCl_2$); $TK_{200}M_7$ (50 mM Tris-HCl [pH 7.5], 200 mM KCl, 7 mM $MgCl_2$); or $T[KGlu]_{100}M_7$ (50 mM Tris-HCl [pH 7.5], 100 mM potassium glutamate, 7 mM $MgCl_2$)).

Time courses of $IF3_{166}$(Alx488) (0.05 μM) binding to increasing concentrations of $50S_{L33}$(Atto540Q) subunits were measured at 4°C (0.05, 0.062, 0.075, 0.087, and 0.1 μM) and 20°C (0.05, 0.075, 0.1, 0.125, and 0.15 μM). IF3 release from the 50S subunits was measured by displacement experiments at 4°C and 20°C in which a pre-incubated mix of $IF3_{166}$(Alx488) (0.15 μM) and $50S_{L33}$(Atto540Q) (0.05 μM) was rapidly mixed with $IF3_{166}$(Alx488) (0.15 μM) and an excess of unlabeled 50S (0.75 μM) or IF3 (1.5 μM). $IF3_{166}$(Alx488) was present in both syringes to ensure that the signal change upon chase did not arise merely due to dilution of the complex. The averages of seven to ten time courses of binding and chase were evaluated using global fitting (one-step model numerical integration) with KinTek Explorer (KinTek) to derive the association and dissociation rate constants.

Fluorescence Anisotropy

Fluorescence anisotropy measurements were performed using a Fluoromax-4 spectrofluorometer (Horiba) in buffers containing 0.1 mg/mL BSA at 20°C. Three technical replicates were recorded for each measurement. Binding of $IF3_{166}$(Alx488) (0.015 μM) to the 50S subunit (0.3 μM) in buffer $TAKM_7$ was monitored by the increase in anisotropy. The emission of Alx488 was measured at 520 nm after excitation at 490 nm. $IF3_{166}$(Alx488) was chased by addition of a 20-fold molar excess of unlabeled IF3 over subunits.

To measure the effect of salt concentration, $IF3_{166}$(Alx488) (0.015 μM) was incubated with 50S subunits (0.3 μM) in buffer $TK_{20}M_7$ (50 mM Tris-HCl [pH 7.5], 20 mM KCl, 7 mM $MgCl_2$) and then increasing amounts of buffered KCl (20 – 220 mM), NaCl (20 – 260 mM), $MgCl_2$ (3 – 70 mM) or KGlu (20 – 260 mM) solutions were added. The change in anisotropy was plotted with respect to the added salt concentration. To monitor the effect of increasing salt on $IF3_{166}$(Alx488) alone, control experiments were performed in the absence of 50S and subtracted from those in the presence of 50S. The corrected data were fit using the equation:

$$Y = y_0 + (y_1\text{-}y_0)/\left(1 + 10^{(\mathrm{Log}(IC50 - x))^{*}k1}\right),$$

where, y_0 = minimum value; y_1 = maximum value; x = log of added salt concentration in M; IC_{50} = inhibitory concentration corresponding to 50% of the amplitude change; k1 = Hill slope factor.

The number of IF3 molecules that bind to the 50S subunit was measured by titrating a fixed concentration of $IF3_{166}$(Alx488) (0.3 μM) with under- and over-stoichiometric amounts of 50S subunits. The change in anisotropy was plotted as a function of 50S concentration. The minimal concentration of 50S that saturated $IF3_{166}$(Alx488) was derived from the intersection between two linear regression fits of the data points as described (Mangel et al., 2016).

SUPPLEMENTAL INFORMATION

Supplemental Information includes three figures and one table and can be found with this article online at http://dx.doi.org/10.1016/j.celrep.2017.09.012.

AUTHOR CONTRIBUTIONS

All authors designed the experiments, analyzed the data, and discussed results; A.G. performed all the experiments, following the initial observation of R.B.; R.B. and A.G. prepared materials; and A.G. and M.V.R. wrote the paper with contributions from R.B.

ACKNOWLEDGMENTS

We thank Dr. Namit Ranjan and Dr. Evan Mercier for critically reading the manuscript; Dr. Pohl Milón for providing preparations of individual IF3 domains and $IF3_{65}$(Alx488); and Olaf Geintzer, Sandra Kappler, Christina Kothe, Anna Pfeifer, Theresia Uhlendorf, Tanja Wiles, Franziska Hummel, and Michael Zimmermann for expert technical assistance. This work was supported by the Max Planck Society and a grant from the Deutsche Forschungsgemeinschaft (SFB860).

Received: July 14, 2017
Revised: August 25, 2017
Accepted: September 3, 2017
Published: September 26, 2017

REFERENCES

Allen, G.S., Zavialov, A., Gursky, R., Ehrenberg, M., and Frank, J. (2005). The cryo-EM structure of a translation initiation complex from Escherichia coli. Cell *121*, 703–712.

Antoun, A., Pavlov, M.Y., Andersson, K., Tenson, T., and Ehrenberg, M. (2003). The roles of initiation factor 2 and guanosine triphosphate in initiation of protein synthesis. EMBO J. *22*, 5593–5601.

Antoun, A., Pavlov, M.Y., Lovmar, M., and Ehrenberg, M. (2006a). How initiation factors maximize the accuracy of tRNA selection in initiation of bacterial protein synthesis. Mol. Cell *23*, 183–193.

Antoun, A., Pavlov, M.Y., Lovmar, M., and Ehrenberg, M. (2006b). How initiation factors tune the rate of initiation of protein synthesis in bacteria. EMBO J. *25*, 2539–2550.

Ayyub, S.A., Dobriyal, D., and Varshney, U. (2017). Contributions of the N- and C-terminal domains of initiation factor 3 to its functions in the fidelity of initiation and antiassociation of the ribosomal subunits. J. Bacteriol. *199*, 199.

Belardinelli, R., Sharma, H., Caliskan, N., Cunha, C.E., Peske, F., Wintermeyer, W., and Rodnina, M.V. (2016). Choreography of molecular movements during ribosome progression along mRNA. Nat. Struct. Mol. Biol. *23*, 342–348.

Berg, O.G., Winter, R.B., and von Hippel, P.H. (1981). Diffusion-driven mechanisms of protein translocation on nucleic acids. 1. Models and theory. Biochemistry *20*, 6929–6948.

Broeze, R.J., Solomon, C.J., and Pope, D.H. (1978). Effects of low temperature on in vivo and in vitro protein synthesis in Escherichia coli and Pseudomonas fluorescens. J. Bacteriol. *134*, 861–874.

Caliskan, N., Katunin, V.I., Belardinelli, R., Peske, F., and Rodnina, M.V. (2014). Programmed -1 frameshifting by kinetic partitioning during impeded translocation. Cell *157*, 1619–1631.

Carter, A.P., Clemons, W.M., Jr., Brodersen, D.E., Morgan-Warren, R.J., Hartsch, T., Wimberly, B.T., and Ramakrishnan, V. (2001). Crystal structure of an initiation factor bound to the 30S ribosomal subunit. Science *291*, 498–501.

Chaires, J.B., Hawley, D.A., and Wahba, A.J. (1982). Chain initiation factor 3 crosslinks to E. coli 30S and 50S ribosomal subunits and alters the UV absorbance spectrum of 70S ribosomes. Nucleic Acids Res. *10*, 5681–5693.

Cravens, S.L., Hobson, M., and Stivers, J.T. (2014). Electrostatic properties of complexes along a DNA glycosylase damage search pathway. Biochemistry *53*, 7680–7692.

Cukras, A.R., and Green, R. (2005). Multiple effects of S13 in modulating the strength of intersubunit interactions in the ribosome during translation. J. Mol. Biol. *349*, 47–59.

Dallas, A., and Noller, H.F. (2001). Interaction of translation initiation factor 3 with the 30S ribosomal subunit. Mol. Cell *8*, 855–864.

Deredge, D.J., Baker, J.T., Datta, K., and Licata, V.J. (2010). The glutamate effect on DNA binding by pol I DNA polymerases: Osmotic stress and the effective reversal of salt linkage. J. Mol. Biol. *401*, 223–238.

Elvekrog, M.M., and Gonzalez, R.L., Jr. (2013). Conformational selection of translation initiation factor 3 signals proper substrate selection. Nat. Struct. Mol. Biol. *20*, 628–633.

Fabbretti, A., Pon, C.L., Hennelly, S.P., Hill, W.E., Lodmell, J.S., and Gualerzi, C.O. (2007). The real-time path of translation factor IF3 onto and off the ribosome. Mol. Cell *25*, 285–296.

Giuliodori, A.M., Brandi, A., Giangrossi, M., Gualerzi, C.O., and Pon, C.L. (2007). Cold-stress-induced de novo expression of infC and role of IF3 in cold-shock translational bias. RNA *13*, 1355–1365.

Goyal, A., Belardinelli, R., Maracci, C., Milón, P., and Rodnina, M.V. (2015). Directional transition from initiation to elongation in bacterial translation. Nucleic Acids Res. *43*, 10700–10712.

Grigoriadou, C., Marzi, S., Kirillov, S., Gualerzi, C.O., and Cooperman, B.S. (2007a). A quantitative kinetic scheme for 70 S translation initiation complex formation. J. Mol. Biol. *373*, 562–572.

Grigoriadou, C., Marzi, S., Pan, D., Gualerzi, C.O., and Cooperman, B.S. (2007b). The translational fidelity function of IF3 during transition from the 30 S initiation complex to the 70 S initiation complex. J. Mol. Biol. *373*, 551–561.

Grunberg-Manago, M., Dessen, P., Pantaloni, D., Godefroy-Colburn, T., Wolfe, A.D., and Dondon, J. (1975). Light-scattering studies showing the effect of initiation factors on the reversible dissociation of Escherichia coli ribosomes. J. Mol. Biol. *94*, 461–478.

Gualerzi, C.O., and Pon, C.L. (1990). Initiation of mRNA translation in prokaryotes. Biochemistry *29*, 5881–5889.

Gualerzi, C.O., and Pon, C.L. (2015). Initiation of mRNA translation in bacteria: Structural and dynamic aspects. Cell. Mol. Life Sci. *72*, 4341–4367.

Guenneugues, M., Caserta, E., Brandi, L., Spurio, R., Meunier, S., Pon, C.L., Boelens, R., and Gualerzi, C.O. (2000). Mapping the fMet-tRNA(f)(Met) binding site of initiation factor IF2. EMBO J. *19*, 5233–5240.

Hirokawa, G., Inokuchi, H., Kaji, H., Igarashi, K., and Kaji, A. (2004). In vivo effect of inactivation of ribosome recycling factor - fate of ribosomes after unscheduled translation downstream of open reading frame. Mol. Microbiol. *54*, 1011–1021.

Hirokawa, G., Kaji, H., and Kaji, A. (2007). Inhibition of antiassociation activity of translation initiation factor 3 by paromomycin. Antimicrob. Agents Chemother. *51*, 175–180.

Howe, J.G., and Hershey, J.W. (1983). Initiation factor and ribosome levels are coordinately controlled in Escherichia coli growing at different rates. J. Biol. Chem. *258*, 1954–1959.

Hussain, T., Llacer, J.L., Wimberly, B.T., Kieft, J.S., and Ramakrishnan, V. (2016). Large-scale movements of IF3 and tRNA during bacterial translation initiation. Cell *167*, 133–144.

Julián, P., Milón, P., Agirrezabala, X., Lasso, G., Gil, D., Rodnina, M.V., and Valle, M. (2011). The Cryo-EM structure of a complete 30S translation initiation complex from Escherichia coli. PLoS Biol. *9*, e1001095.

Koldewey, P., Stull, F., Horowitz, S., Martin, R., and Bardwell, J.C.A. (2016). Forces Driving Chaperone Action. Cell *166*, 369–379.

Korennykh, A.V., Piccirilli, J.A., and Correll, C.C. (2006). The electrostatic character of the ribosomal surface enables extraordinarily rapid target location by ribotoxins. Nat. Struct. Mol. Biol. *13*, 436–443.

Kycia, J.H., Biou, V., Shu, F., Gerchman, S.E., Graziano, V., and Ramakrishnan, V. (1995). Prokaryotic translation initiation factor IF3 is an elongated protein consisting of two crystallizable domains. Biochemistry *34*, 6183–6187.

Laursen, B.S., Sørensen, H.P., Mortensen, K.K., and Sperling-Petersen, H.U. (2005). Initiation of protein synthesis in bacteria. Microbiol. Mol. Biol. Rev. *69*, 101–123.

Leirmo, S., Harrison, C., Cayley, D.S., Burgess, R.R., and Record, M.T., Jr. (1987). Replacement of potassium chloride by potassium glutamate dramatically enhances protein-DNA interactions in vitro. Biochemistry *26*, 2095–2101.

Liu, Q., and Fredrick, K. (2015). Roles of helix H69 of 23S rRNA in translation initiation. Proc. Natl. Acad. Sci. USA *112*, 11559–11564.

MacDougall, D.D., and Gonzalez, R.L., Jr. (2015). Translation initiation factor 3 regulates switching between different modes of ribosomal subunit joining. J. Mol. Biol. *427*, 1801–1818.

Mangel, W.F., McGrath, W.J., Xiong, K., Graziano, V., and Blainey, P.C. (2016). Molecular sled is an eleven-amino acid vehicle facilitating biochemical interactions via sliding components along DNA. Nat. Commun. *7*, 10202.

Meneses, E., and Mittermaier, A. (2014). Electrostatic interactions in the binding pathway of a transient protein complex studied by NMR and isothermal titration calorimetry. J. Biol. Chem. *289*, 27911–27923.

Menetski, J.P., Varghese, A., and Kowalczykowski, S.C. (1992). The physical and enzymatic properties of Escherichia coli recA protein display anion-specific inhibition. J. Biol. Chem. *267*, 10400–10404.

Milón, P., and Rodnina, M.V. (2012). Kinetic control of translation initiation in bacteria. Crit. Rev. Biochem. Mol. Biol. *47*, 334–348.

Milón, P., Konevega, A.L., Peske, F., Fabbretti, A., Gualerzi, C.O., and Rodnina, M.V. (2007). Transient kinetics, fluorescence, and FRET in studies of initiation of translation in bacteria. Methods Enzymol. *430*, 1–30.

Milón, P., Konevega, A.L., Gualerzi, C.O., and Rodnina, M.V. (2008). Kinetic checkpoint at a late step in translation initiation. Mol. Cell *30*, 712–720.

Milón, P., Carotti, M., Konevega, A.L., Wintermeyer, W., Rodnina, M.V., and Gualerzi, C.O. (2010). The ribosome-bound initiation factor 2 recruits initiator tRNA to the 30S initiation complex. EMBO Rep. *11*, 312–316.

Milón, P., Maracci, C., Filonava, L., Gualerzi, C.O., and Rodnina, M.V. (2012). Real-time assembly landscape of bacterial 30S translation initiation complex. Nat. Struct. Mol. Biol. *19*, 609–615.

Mohapatra, S., Choi, H., Ge, X., Sanyal, S., and Weisshaar, J.C. (2017). Spatial distribution and ribosome-binding dynamics of EF-P in live Escherichia coli. MBio *8*, 8.

Moll, I., Hirokawa, G., Kiel, M.C., Kaji, A., and Bläsi, U. (2004). Translation initiation with 70S ribosomes: An alternative pathway for leaderless mRNAs. Nucleic Acids Res. *32*, 3354–3363.

Moreau, M., de Cock, E., Fortier, P.L., Garcia, C., Albaret, C., Blanquet, S., Lallemand, J.Y., and Dardel, F. (1997). Heteronuclear NMR studies of E. coli translation initiation factor IF3. Evidence that the inter-domain region is disordered in solution. J. Mol. Biol. *266*, 15–22.

Pavlov, M.Y., Zorzet, A., Andersson, D.I., and Ehrenberg, M. (2011). Activation of initiation factor 2 by ligands and mutations for rapid docking of ribosomal subunits. EMBO J. *30*, 289–301.

Petrelli, D., LaTeana, A., Garofalo, C., Spurio, R., Pon, C.L., and Gualerzi, C.O. (2001). Translation initiation factor IF3: Two domains, five functions, one mechanism? EMBO J. *20*, 4560–4569.

Rodnina, M.V., Pape, T., Fricke, R., and Wintermeyer, W. (1995). Elongation factor Tu, a GTPase triggered by codon recognition on the ribosome: Mechanism and GTP consumption. Biochem. Cell Biol. *73*, 1221–1227.

Ruscetti, F.W., and Jacobson, L.A. (1972). Accumulation of 70S monoribosomes in Escherichia coli after energy source shift-down. J. Bacteriol. *111*, 142–151.

Saecker, R.M. (2007). Protein-DNA complexes: Nonspecific. In eLS (John Wiley & Sons).

Schwartz, I., Vincent, M., Strycharz, W.A., and Kahan, L. (1983). Photochemical cross-linking of translation initiation factor 3 to Escherichia coli 50S ribosomal subunits. Biochemistry *22*, 1483–1489.

Sette, M., van Tilborg, P., Spurio, R., Kaptein, R., Paci, M., Gualerzi, C.O., and Boelens, R. (1997). The structure of the translational initiation factor IF1 from E.coli contains an oligomer-binding motif. EMBO J. *16*, 1436–1443.

Simonetti, A., Marzi, S., Myasnikov, A.G., Fabbretti, A., Yusupov, M., Gualerzi, C.O., and Klaholz, B.P. (2008). Structure of the 30S translation initiation complex. Nature *455*, 416–420.

Spurio, R., Brandi, L., Caserta, E., Pon, C.L., Gualerzi, C.O., Misselwitz, R., Krafft, C., Welfle, K., and Welfle, H. (2000). The C-terminal subdomain (IF2 C-2) contains the entire fMet-tRNA binding site of initiation factor IF2. J. Biol. Chem. *275*, 2447–2454.

Tomsic, J., Vitali, L.A., Daviter, T., Savelsbergh, A., Spurio, R., Striebeck, P., Wintermeyer, W., Rodnina, M.V., and Gualerzi, C.O. (2000). Late events of translation initiation in bacteria: A kinetic analysis. EMBO J. *19*, 2127–2136.

Uchida, T., Abe, M., Matsuo, K., and Yoneda, M. (1970). Different sensitivity to ribonuclease of complexed and free ribosome. Biochim. Biophys. Acta *224*, 628–630.

Wang, J., Caban, K., and Gonzalez, R.L., Jr. (2015). Ribosomal initiation complex-driven changes in the stability and dynamics of initiation factor 2 regulate the fidelity of translation initiation. J. Mol. Biol. *427*, 1819–1834.

Weiel, J., and Hershey, J.W. (1981). Fluorescence polarization studies of the interaction of Escherichia coli protein synthesis initiation factor 3 with 30S ribosomal subunits. Biochemistry *20*, 5859–5865.

Yamamoto, H., Wittek, D., Gupta, R., Qin, B., Ueda, T., Krause, R., Yamamoto, K., Albrecht, R., Pech, M., and Nierhaus, K.H. (2016). 70S-scanning initiation is a novel and frequent initiation mode of ribosomal translation in bacteria. Proc. Natl. Acad. Sci. USA *113*, E1180–E1189.

Zorzet, A., Pavlov, M.Y., Nilsson, A.I., Ehrenberg, M., and Andersson, D.I. (2010). Error-prone initiation factor 2 mutations reduce the fitness cost of antibiotic resistance. Mol. Microbiol. *75*, 1299–1313.

Cell Reports, Volume *20*

Supplemental Information

Non-canonical Binding Site for Bacterial Initiation Factor 3 on the Large Ribosomal Subunit

Akanksha Goyal, Riccardo Belardinelli, and Marina V. Rodnina

Supplemental Materials

Table S1. Summary of the apparent rate constants of subunit joining and FRET changes during 70S IC formation. Related to Figures 1 and S3.

FRET pair	Light scattering (SJ, GTP)[a] k_{app} (s^{-1})	FRET (SJ, GTP)[b] k_{app} (s^{-1})	FRET (SJ, GTPγS)[c] k_{app} (s^{-1})	FRET (chase, GTP)[d] k_{app} (s^{-1})
$IF1_4$(Atto540Q) - $IF3_{166}$(Alx488)	5.8 ± 0.4 (45 %) 0.8 ± 0.1 (55 %)	4.8 ± 0.3 (20 %) 1.0 ± 0.1 (70 %)	4.9 ± 0.3 (19 %) 1.1 ± 0.1 (65 %)	5.6 ± 0.5 (88 %)
$IF2_{757}$(Atto540Q) - $IF3_{166}$(Alx488)	5.9 ± 0.5 (48 %) 1.0 ± 0.1 (52 %)	4.2 ± 0.3 (32 %) 1.0 ± 0.1 (68 %)	3.7 ± 0.3 (38 %) 0.9 ± 0.1 (62 %)	6.0 ± 0.5 (80 %)
$30S_{S13}$(Alx488) - $IF3_{166}$(Atto540Q)	0.43 ± 0.05 (57 %) 0.012 ± 0.002 (43 %)	0.40 ± 0.05 (62%) 0.04 ± 0.01 (24 %)	0.36 ± 0.04 (58%) 0.03 ± 0.01 (26 %)	2.9 ± 0.3 (55%) 0.4 ± 0.1 (36 %)
$50S_{L33}$(Atto540Q) - $IF3_{166}$(Alx488)	1.9 ± 0.1 (34 %) 0.24 ± 0.04 (45 %)	1.2 ± 0.1 (83%)	1.3 ± 0.1 (100%)	n.d.

[a,b,c]0.05 μM 30S IC (formed using different fluorescence-labeled components) was mixed with 0.15 μM 50S subunits. SJ – subunit joining. In [b,c] FRET time courses were corrected by subtracting the donor fluorescence. All rates are derived from exponential fittings of time courses.

[d]0.05 μM 30S IC (formed using different fluorescence-labeled components) was mixed with 1.5 μM unlabeled IF3.

Rate values are represented as mean ± s.e.m; n.d. – not determined. Amplitude contributions of the dominant phases (comprising greater than 80 % amplitude change) are indicated in brackets.

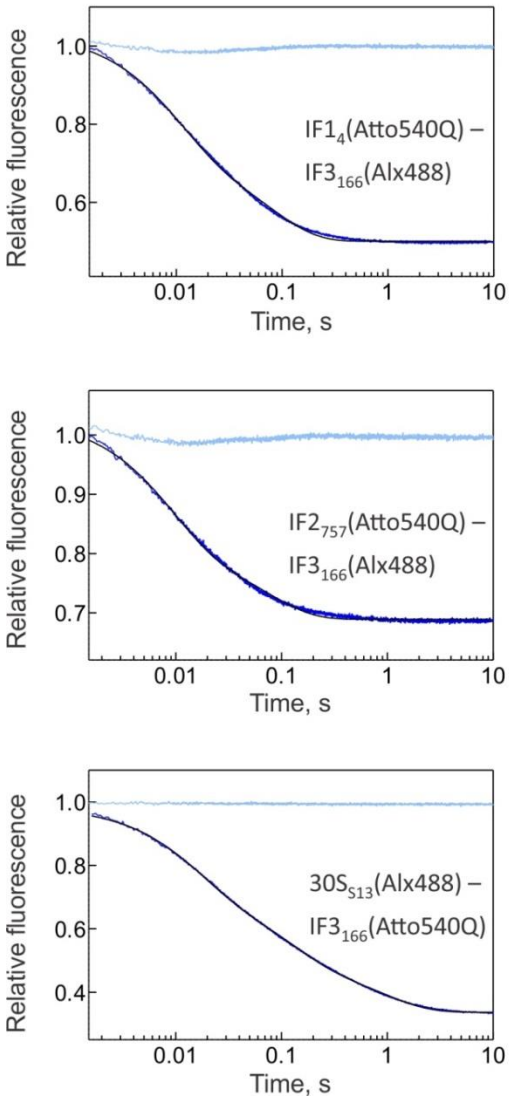

Figure S1. FRET changes upon IF3 binding to 30S PIC. Related to Figure 1.

Labeled 30S PIC (lacking IF3) (0.05 μM) were rapidly mixed with labeled IF3 (0.05 μM) and FRET changes between the indicated components were monitored with time (blue). Control experiments were performed in the absence of the acceptor dye (light blue). Black smooth lines represent exponential fitting of time courses. All reactions were performed in buffer TAKM$_7$ at 20°C.

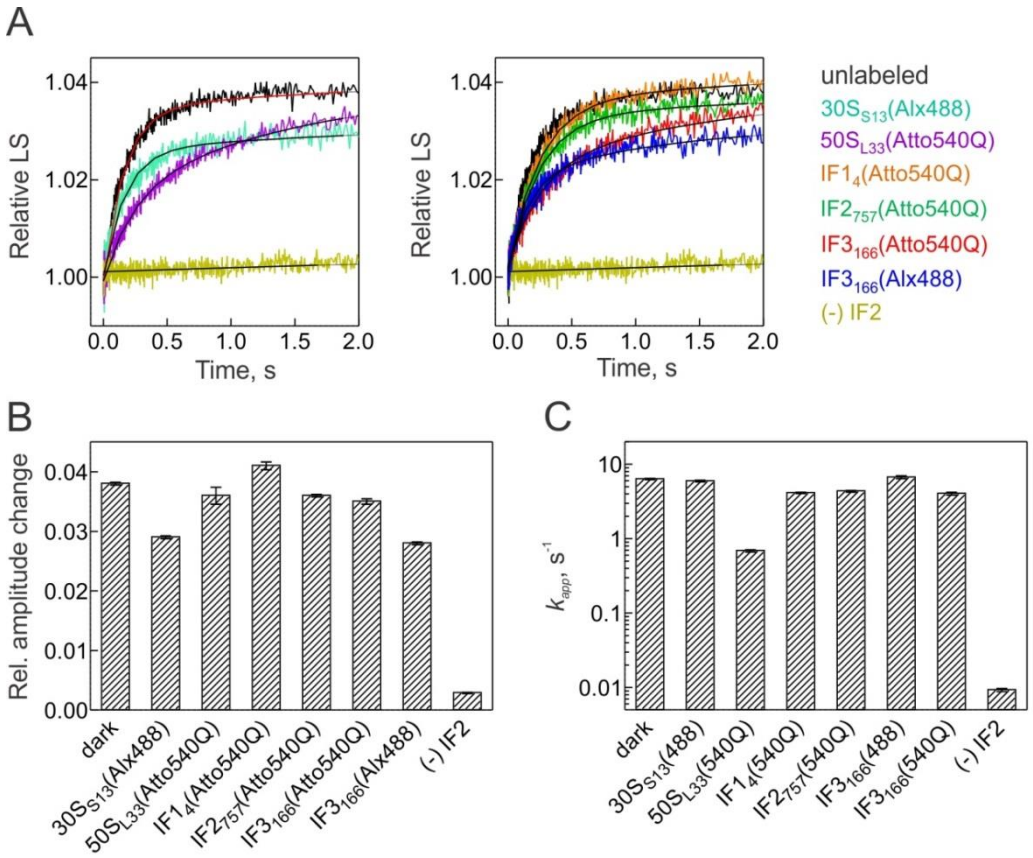

Figure S2. Activity of labeled ribosomal subunits and IFs. Related to Figure 1.

(A) 30S IC formed using indicated fluorescent components (0.05 μM) were rapidly mixed with 50S subunits (0.25 μM) and subunit association was monitored via changes in light scattering (LS). Positive and negative control measurements performed in the absence of any fluorescent label (black) or IF2 (gold), respectively, are depicted in both panels for comparison. Black smooth lines represent double-exponential fits of time courses.

(B-C) The relative change in amplitude at 2 s and the apparent rate of the predominant phase derived from double-exponential fitting of time courses in (A), respectively; error bars represent the standard error of the fit. All reactions were performed in buffer $TAKM_7$ at 20°C.

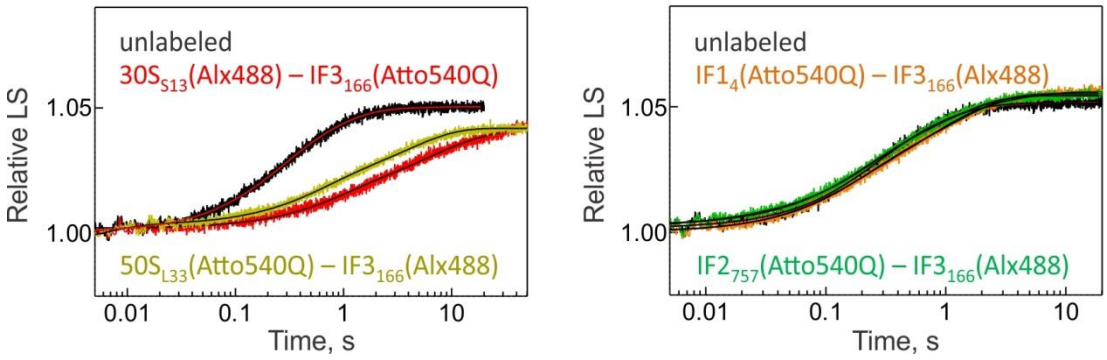

Figure S3. Kinetics of subunit joining monitored with different FRET pairs. Related to Figure 1.

30S IC formed in the presence of indicated components (0.05 μM) were rapidly mixed with 50S subunits (0.15 μM) and subunit joining was monitored with time. The same control measurement performed in the absence of any fluorescent label (black), is depicted in both panels for visual comparison. Fits derived from exponential fitting of time courses are shown as black smooth lines (see Table S1 for rates). All reactions were performed in buffer TAKM$_7$ at 20°C.